

## Design and Analysis of Vertical Axis Wind Turbine Blades for Street Lighting

<sup>1</sup> Madhura Yeligeti, Ganesh Shete<sup>2</sup>, Prateek Tade<sup>3</sup>, Prof. Sachin Vankar<sup>4</sup><sup>1</sup>Student, Mechanical Engineering Dept., Sardar Patel College of Engineering, India, madhurayeligeti@gmail.com<sup>2</sup>Student, Mechanical Engineering Dept., Sardar Patel College of Engineering, India, ganesh.shete@hotmail.com<sup>3</sup>Student, Mechanical Engineering Dept., Sardar Patel College of Engineering, India, prateek.tade@gmail.com<sup>4</sup>Faculty, Mechanical Engineering Dept., Sardar Patel College of Engineering, India, sachin@spce.ac.in**ABSTRACT**

With a view to harnessing wind energy in small application, a design of a vertical axis Savonius – Darrieus integrated Wind Turbine is proposed to be mounted on a Streetlight pole. Important aspects about street lighting and wind data are discussed. The blade geometry (Troposkein shape) for the Darrieus rotor is approximated by an iterative method. The entire Design process is performed for two materials: Aluminum Alloy and E- glass Fiber. The aerodynamic forces are calculated on Darrieus blade and Savonius rotors stress analysis is performed on them. A computational fluid dynamics (CFD) tool (ANSYS Fluent) is used on Savonius blade for aerodynamic analysis. ANSYS Static Structural software is used for stress analysis.

**Key words :** Darrieus rotor, E-glass fiber, Savonius rotor, S –C –S Approximation of Troposkein shape, Street lighting

**1. INTRODUCTION**

Wind power, today is harnessed typically in wind farms consisting of massive windmills, mostly horizontal axis wind turbines (HAWTs). Wind turbines with vertical rotating axis are not so popular because of their less efficiency and stability characteristics. However, these vertical axis wind turbines (VAWTs) can be used effectively in small-scale applications like electricity generation for homes, offices, malls, etc. Small VAWTs installed in large numbers can reduce the dependency on conventional energy resources substantially.

The original Vertical Axis Wind Turbine is the Darrieus turbine as shown in Figure 1. It is a lift type turbine. It has comparatively high efficiency, but self-starting ability is less. The Savonius turbine (Figure 2) is a drag type turbine. The efficiency of this turbine is very less (0.20-0.30).

The high power efficiency of the Darrieus turbine and the self-starting ability of the Savonius Turbine can be brought together by integrating the two rotors on the same shaft. In this design, we use such a combination of Darrieus and Savonius Turbine on a streetlight pole. (Figure 3)



Figure 1: Darrieus wind turbine [1]



Figure 2: Savonius wind turbine [2]

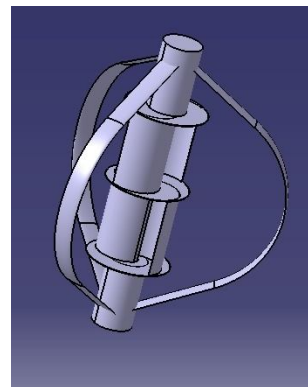


Figure 3: Darrieus Savonius integrated turbine

## 2. STREET LIGHTING

According to IS: 1944 (part 1-6), the road condition is a decisive factor in determining street lights. Lighting can be classified into the groups A1, A2, B1, B2, C, D, E and F [3]. As a general norm, heights of 9-10 metres are suitable for Group A roads and 7.5 to 9 metres for Group B roads.

In this paper, the lighting conditions are taken for Group B roads with a street light pole of 8 metres. Considering a dual lamp system on Group B type road with LED lighting, we consider a power requirement of **100 watts** and proceed with the design. The turbine will be mounted at a height of about **9 meters** from the ground.

## 3. WIND DATA

In MUMBAI, typical wind speeds vary from 0 m/s to 6m/s throughout the year rarely exceeding 9 m/s. Mean established wind speed in this period is merely 10 km/ hr (2.78 m/s). [4] The wind speed data for Mumbai region around Juhu measured from January 2008 to February 2016 during the day timings from 7:00 a.m. to 7:00 p.m. is given in figure 4.

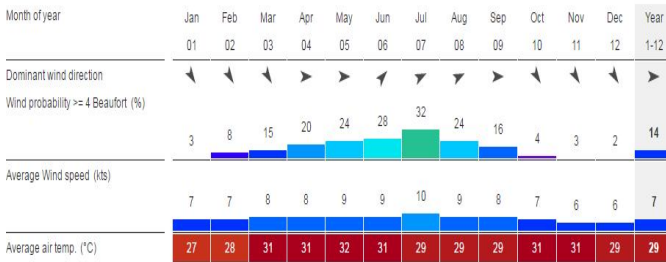


Figure 4: Wind speed data in Juhu region (2008-2016) [6]

Table 1: Relationship between wind speed and wind potential [5]

Mean Wind Speed at 10 m Height (m/s)	Indicated Value of Wind Resource
< 4.5	Poor
4.5 - 5.4	Marginal
5.4 - 6.7	Good to very Good
> 6.7	Exceptional

The Table 1 shows the relationship between wind speed and wind energy potential.

The above information clearly shows that the city of Mumbai has a low potential for wind energy utilization. However, given the nature of vertical axis wind turbine, its low speed requirement; the low power requirement for the LED Street Lighting System, the proposed design is a feasible and in fact, a reliable alternative.

## 4. DESIGN OF DARRIEUS TURBINE

### 4.1 Material considerations

In Darrieus turbines usually, the structural components are made of steel or such other ferrous alloys. The most predominant material used in blades is aluminium. **Aluminium alloys** have been used particularly because of their light weight, less density, corrosion and abrasion resistance, ease of availability and low cost

Aluminium material used in blades is extruded and bent to give it the blade shape.. Aluminium alloys used in turbine blades have mechanical properties like Young’s modulus =72 GPa, density = 2770 kg/m<sup>3</sup> and ultimate tensile strength of approximately 310 MPa. However, its major drawback is the low fatigue strength.

The Vertical Axis Wind Turbines face extreme cyclic loading conditions and induce centrifugal and aerodynamic stresses. Aluminium not only has poor fatigue properties hence, an alternative material is also considered in this design.

Some materials that can be potentially used in wind turbines are as under:

- **Wood and Wood Epoxy:** Wood has been a popular option in ancient times for turbine blades. Douglas fir can be used in blades and structural components since they have high tensile strength. [8] Instead of the entire blade being made out of wood, wood fibres are used in composites, instead of carbon or other materials.
- **Fiber glass composites / Glass Fiber Reinforced Plastic (Glass FRP):** Fiberglass is typically used for its high mechanical strength, cost-effectiveness, light weight and resistance to corrosion and thermal stress. [10]

E-glass FRP typically has a density around 2580 kg/m<sup>3</sup>, Young’s modulus 73-84 GPa, an Ultimate Tensile Strength of approximately 2000 MPa. E-glass is manufactured with a unique process called pultrusion. In turbine applications, E-glass is typically made in an epoxy, polyester or vinyl ester matrix. [8]

- **Carbon Fiber reinforced plastic:** Carbon Fibers are stronger and have more stiffness than glass fibers. One innovative use of carbon fibers is to use them in conjunction with glass fibers in reinforced plastic, to get the advantage of strength and reduced cost. [7]

The alternative material considered here is E-Glass FRP.

### 4.2 Geometric considerations

According to a numerical analysis [11] a suitable tradeoff between normal force and power efficiency has to be considered for determining the number of blades and the chord length in our Darrieus rotor.

For a two blade system the blades are oriented 180 degrees apart. There is a large cyclic variation in both magnitude and direction of the aerodynamic forces on a two blade rotor, which is a major problem especially in small turbines. On the other hand, the force and the torque are steady on a three blade rotor which are oriented at a 120 degree angle from each other. [12]

When the number of blades increases above 3 or 4, the maximum power coefficient attained decreases. Thus, considering the above factors, the number of blades chosen here is three.

**4.2.1 Aerofoil section**

Some typical airfoils used in Wind Turbines are: NACA 0012, NACA 0015, NACA 4415 and NACA 23012

NACA 0012 and NACA 0015 are symmetrical aerofoils. Besides, these are also comparatively thin aerofoils. The aerofoil NACA 0012 has high lift to drag ratio [14].

In this analysis, we have selected the NACA 0012 aerofoil sections for the blade profile. The co-ordinates of the profile were imported into CATIA software while modeling the blade. Considering the turbine size, the blade chord length is taken as 100 mm.

**4.2.2 Type of turbine model**

In the Darrieus 'EGG-BEATER' model the curve formed by the blades is termed as the 'Troposkein' curve.. The troposkein is an ideal shape of the turbine blades with zero bending stresses on account of rotation. For manufacturing considerations, Troposkein is approximated to various shapes. The closest approximation, as proposed by Sandia National Laboratories [13], is that of a straight-circular-straight (SCS) shape, also called the Sandia Curve. This shape consists of a circular arc at the centre and straight lines at the top and bottom tangential to the arc at both of its ends.

**4.2.3 Aspect ratio ( $\beta$ )**

The aspect ratio is an important design parameter that influences the performance of a turbine. According to one of Sandia Laboratories' Research [15] the best S-C-S approximation for Troposkein was obtained at  $\beta = 0.9945608 \approx 1.00$ . Thus, this design proceeds with an aspect ratio of 1.00.

Considering, the size of the streetlight pole, the height of the turbine should be in the range of 0.75-2.0 metres. So,we consider the maximum radius as 0.7 metres. This implies that the semi-height is also 0.7 m and the height of the turbine blades is 1.4 m. Note that the total height of the turbine above the pole will be greater than 1.4 m. The basic design data of the Darrieus blade is summarized in table 2.

**4.2.4 Iterative blade geometry determination using stress calculation**

We have adopted this iterative stress calculation method to determine the best S-C-S approximation (Sandia Shape). This method analyses the centrifugal stresses induced for various approximations using the ANSYS (Static Structural) Software. The criterion for goodness of fit is the least maximum stresses induced because of rotation about the shaft axis.

**Table 2:** Darrieus blade specifications

Sr. No.	Specification	Value / Description
1	Material	Aluminium Alloy/ E-Glass Fiber reinforced Plastic
2	No. of blades in turbine	3
3	Blade Profile	NACA 0012
4	Chord Width	100 mm
5	Maximum Radius of rotor	0.7 m
6	Height of rotor (total )	1.4 m
7	Blade Shape	Sandia ( S-C-S ) Curve

For the various geometries to be checked, we will consider an **R versus Z** co-ordinate system, on a single blade as shown in **Figure 5**. The R-axis is along its radial centerline, while the X-axis is along the vertical centerline.

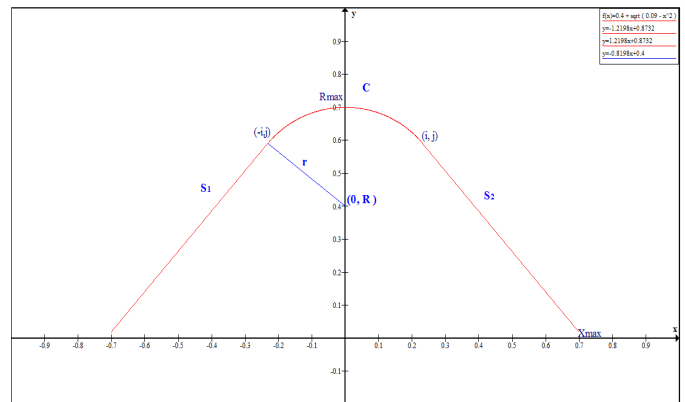


**Figure 5:** Details of S-C-S approximation for Darrieus wind turbine

- $S_1$  and  $S_2$  : Straight Line Segments
- $C$  : Circular Arc
- $R_{max}$  = Maximum radius (of turbine)
- $X_{max}$  = Semi-height
- $(0, R)$  = Centre of arc  $C$
- $r$  = Radius of the arc  $C$
- $(i, j)$  and  $(-i, j)$  : Coordinates of Nodal points {i.e. the points at which the lines  $S_1$  and  $S_2$  meet the arc  $C$  respectively}

#### 4.2.4.1 Derivation of equations

On account of the symmetry about R-axis, the equations are derived only for the positive R-X axes. From this, the coordinates for S<sub>1</sub> too can be easily calculated.

Equation of circle at center (0, R) and radius ‘r’ is given as:

$$x^2 + (y - R)^2 = r^2$$

To simplify our calculation, let us shift the origin to (0, R) Therefore, in the new frame of co-ordinates, the equation of the arc (circle) is

$$x^2 + y^2 = r^2 \dots \dots \dots (1)$$

Let the equation of line S<sub>2</sub> in this reference frame be

$$y = mx + c \dots \dots \dots (2)$$

For x = 0.7, y = - R ∴ -R = 0.7m + c

$$\therefore c = -R - 0.7m \dots \dots \dots (3)$$

From (1) and (2), we get

$$x^2 + (mx + c)^2 = r^2$$

$$\therefore x^2 + m^2x^2 + 2cmx + c^2 = r^2$$

$$\therefore x^2(1 + m^2) + 2cmx + c^2 - r^2 = 0$$

Since Line S<sub>2</sub> is tangent to the arc, the above equation will have only one root. Hence, the discriminant Δ is zero.

$$\therefore 4c^2m^2 - 4(1 + m^2)(c^2 - r^2) = 0$$

This gives:

$$m^2r^2 - c^2 + r^2 = 0$$

Substituting c from equation (3), we get

$$m^2r^2 - (-R - 0.7m)^2 + r^2 = 0$$

$$m^2(0.49 - r^2) + 1.4Rm + (R^2 - r^2) = 0$$

This is a quadratic equation in m, hence we get

$$m = \frac{-1.4R \pm \sqrt{(1.4R)^2 - 4(0.49 - r^2)(R^2 - r^2)}}{2(0.49 - r^2)}$$

$$\therefore m = \frac{-1.4R \pm r\sqrt{4R^2 + 1.96 - 4r^2}}{2(0.49 - r^2)}$$

This will give two values of m: m<sub>1</sub> and m<sub>2</sub>. We select the lesser one of the two. That is m = min (m<sub>1</sub>, m<sub>2</sub>)

From the values of m, c can be calculated as per equation (3). The values of i and j in the global reference plane can be obtained as:

$$i = \frac{-mc}{(1 + m^2)}$$

$$C = c + R$$

$$j = m i + C$$

Let the angle included by the arc be θ

This can be obtained as

$$\theta = 2 \{ 90 - (\tan^{-1} (j - R) / x_c) \}$$

#### 4.2.4.2 Sample calculation

R = 0.5 m, r = 0.2 m

$$\therefore c = 0.7m - 0.5$$

$$m = \frac{(-1.4)(0.5) - 0.2\sqrt{1.96 + 4(0.25 - 0.04)}}{2(0.49 - 0.04)}$$

This gives m = -1.1496 and c = 0.3047

From this, we get

$$i = \frac{-(-1.1496) \times (0.3047)}{(1 + 1.1496^2)}$$

Thus, i = 0.1509 m, j = 0.6312 m

Included angle

$$\theta = 2 \times \{ 90 - \tan^{-1} (0.6312 - 0.5) / 0.1509 \}$$

We get θ = 97.99°

These values are used to model the blade in CATIA as shown in **Figure 6**. In this way, the values required to calculate different approximations are calculated and summarized in **Table 3**.

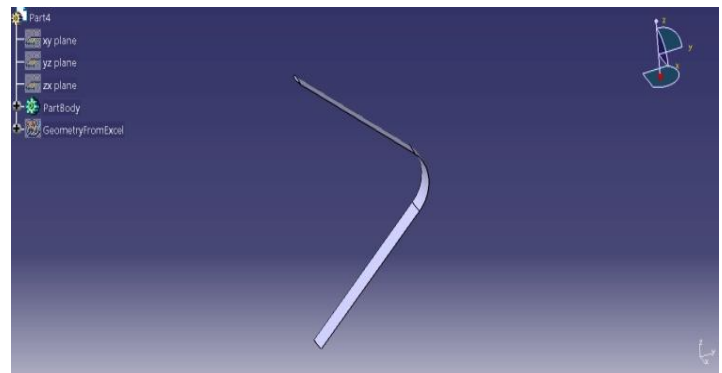


**Figure 6:** CAD model of blade at r=0.2 in CATIA

Further, each model is imported in ANSYS Static Structural and checked for normal stress and strain.

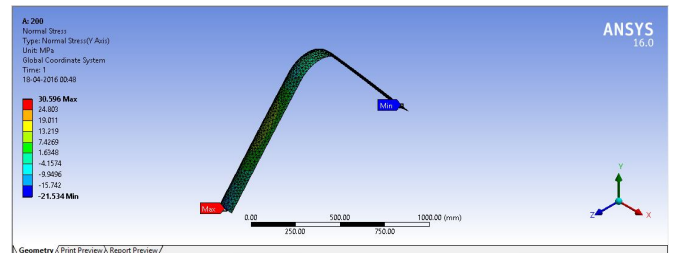


**Figure 7:** Normal stresses (force towards shaft axis) on aluminium blade for r=0.2 m

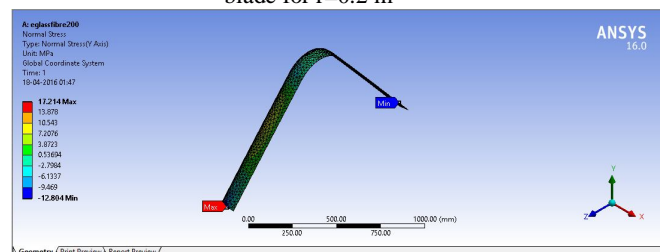


**Figure 8:** Normal stresses (force towards shaft axis) on E-glass FRP r=0.2 m blade

**Table 3:** Summary of calculations for S-C-S approximation

Sr. No	Centre of Arc (0,R)	Radius of Arc r (meters)	Nodal Point of S <sub>2</sub> & Arc C		Included Angle Θ°
			I	j	
1.	(0,0)	0.7	0.7	0	180°
2.	(0,0.1)	0.6	0.5489	0.3422	132.38°
3.	(0,0.2)	0.5	0.4300	0.4550	118.66°
4.	(0,0.3)	0.4	0.3272	0.5300	109.79°
5.	(0,0.4)	0.3	0.2320	0.5860	102.56°
6.	(0,0.5)	0.2	0.1509	0.06312	97.99°
7.	(0,0.6)	0.1	0.0729	0.6684	93.65°
8.	(0,0.55)	0.15	0.1112	0.6506	95.73°
9.	(0,0.45)	0.25	0.1921	0.6100	100.42°
10.	(0,0.35)	0.35	0.2799	0.5600	106.24°
11.	(0,0.25)	0.45	0.3770	0.4957	113.81°
12.	(0,0.27)	0.43	0.3567	0.5101	112.11°
13.	(0,0.23)	0.47	0.3977	0.4803	115.63°

A graph was plotted indicating the various iterative approximations taken and the corresponding normal bending stresses (refer **Figure 9** and **Figure 10**).

From the above graphs, it is clear that the best approximation is when the radius of the arc is **500mm** i.e. r = 0.5 m. With this blade geometry, the blade is designed and taken for further analysis.

**4.3 Aerodynamic analysis of design**

The point where the power coefficient is maximum is called as the optimum tip speed ratio For 3 blades and NACA 0012 the optimum tip speed ratio is slightly more than 4 [16]. Hence, this design analysis is based on the consideration that the tip speed ratio is 4.00 at the maximum distance from the shaft axis.

**4.3.1 Derivation of lift and drag forces**

Let velocity of wind be v m/s  
 Tip speed ratio = λ  
 Peripheral velocity = u m/s

The lift and drag forces because of the wind on the blade are shown in **Figure 11**.

The relative wind velocity v<sub>R</sub> can be calculated in magnitude as [10] :

$$v_R = v\sqrt{(\lambda + \cos \varphi)^2 + (\sin \varphi)^2}$$

where φ: azimuthal angle, i.e. angle in the horizontal plane of the blade, varies from 0° to 360°

The lift and drag forces F<sub>L</sub> and F<sub>D</sub> as shown in **Figure 11** depend on the angle of attack α, which is a function of φ and the tip speed ratio λ. [10]

$$\alpha = \tan^{-1} \left[ \frac{\sin \varphi}{(\lambda + \cos \varphi)} \right]$$

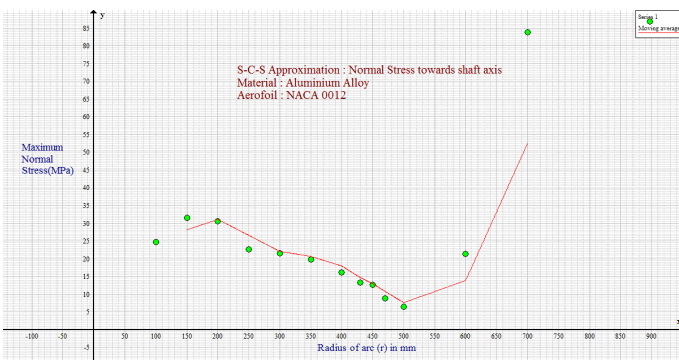


**Figure 9:** Graph of normal stress v/s iterative models (aluminium alloy)

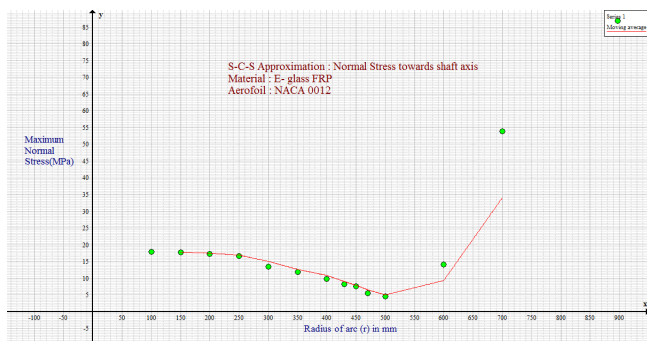


**Figure 10:** Graph of normal stress v/s iterative models (E-glass FRP)

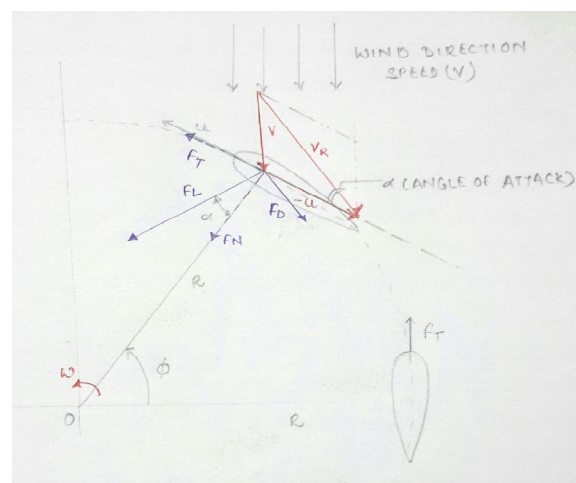


**Figure 11:** Forces acting on aerofoil

$\alpha$  can be either positive or negative. When  $\alpha=0$ , the blades have no lift force at that instant, i.e. they do not produce energy. In fact, the drag force pushes them in the opposite direction. However, since the number of blades is 3, the angle of attack  $\alpha$  does not become zero for all the blades at the same time. Hence, at least some lift is produced to keep the turbine moving.

The magnitude of the lift and drag force induced in the blade is given as [9]

$$F_L = C_L \times \frac{1}{2} \rho A v_R^2$$

$$F_D = C_D \times \frac{1}{2} \rho A v_R^2$$

where

- $C_L$ : lift coefficient
- $C_D$ : drag coefficient
- P: density of air
- A: swept area of the turbine

where the values of  $C_L$  and  $C_D$  vary with the angle of attack  $\alpha$  and represent the characteristics of the aerofoil for different Reynolds numbers (Re).

[14] gives details of the lift and drag coefficients for NACA 0012 airfoil at angles of attack  $0^\circ$ - $180^\circ$  for a wide range of Reynolds numbers ( $10^4$ - $10^7$ ).

The forces  $F_L$  and  $F_D$  can be divided into tangential and normal components of force  $F_T$  and  $F_N$  respectively as [9]:

$$F_T = F_L \sin \alpha - F_D \cos \alpha$$

$$F_N = F_L \cos \alpha + F_D \sin \alpha$$

The tangential force  $F_T$  causes the motion of the blades and gives the torque

$$M_t = F_T \times R$$

The normal force  $F_N$  acts on the structure and induces stresses.

Note that as  $\phi$  changes throughout the rotation,  $\alpha$  changes from positive to negative. The values of normal force  $F_N$  for any  $\alpha$  and  $(-\alpha)$  are the same, only the direction is opposite. Hence, analysis is done for both direction of forces. The following calculations only consider the positive values of  $\alpha$  for estimating the values of  $F_T$  and  $F_N$ .

Also,  $C_L$  and  $C_D$  vary with  $\alpha$ . The tip speed ratio  $\lambda$  varies throughout the blade profile at any instant. Hence to make the calculations simpler, only a few critical values of  $\alpha$  are selected for further calculations.

#### 4.3.1.1 Calculations

- Wind speed ( $v$ ) = 6 m/s
- Tip speed ratio ( $\lambda$ ) = 4
- Density of air at 30C ( $\rho$ ) = 1.164 kg/m<sup>3</sup>
- Swept area (A) = 1.3266 m<sup>2</sup> (refer **Figure 12**)

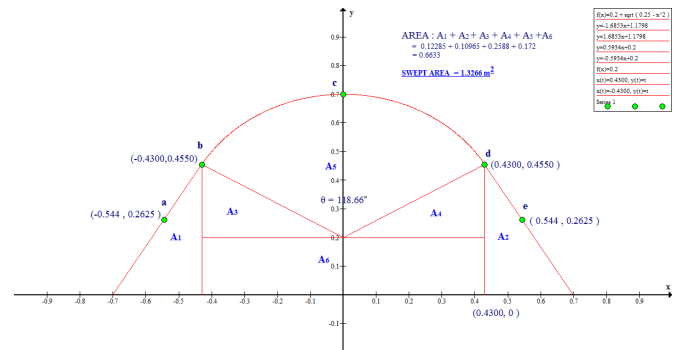


**Figure 12:** Swept area of  $r=0.2$  Darrieus blade

Since  $\lambda$  varies across the blade profile, so do other parameters. Hence we select 5 such points a, b, c, d, e distributed over the blade profile (Refer **Figure 12**) for analysis.

At point a (-0.544, 0.2625) and e (0.544, 0.2625), the tip speed ratio  $\lambda = 1.5$ .

At point b (-0.4300, 0.4550) and d (0.4300, 0.4550) (b & d are nodal points),  $\lambda = 2.6$ .

[ $\lambda$  values are calculated taking  $\lambda = 4$  at point c.

$$\text{This gives } RPM = \frac{4 \times 6 \times 60}{\pi \times 1.4}$$

Hence rotational velocity of turbine = 327.40 rpm]

For  $\lambda = 4$ ,  $\lambda = 2.6$ ,  $\lambda = 1.5$  the values of  $\alpha$  w.r.t.  $\phi$  are as shown in **Figure 13**.

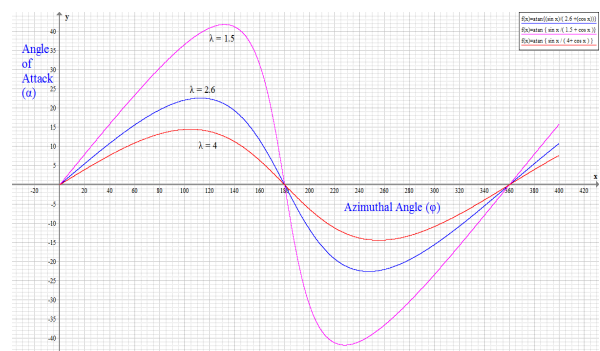


**Figure 13:** Graph of angle of attack ( $\alpha$ ) v/s azimuthal angle ( $\phi$ )

The optimum tip speed ratio ( $\lambda=4$ ) is obtained at a moderate Reynolds number [17]. Thus we select the values of lift and drag coefficients at  $Re=10^6$ .

From the data obtained [14], a graph is plotted taking the point-wise mean for  $\alpha$  values from  $0^\circ$  to  $45^\circ$  as shown in **Figure 14** and **Figure 15**. The values of  $\alpha$  for different critical azimuthal angles at different  $\lambda$  are given in **Table 4**. The values of tangential and normal forces are calculated for different azimuthal angles as shown in **Table 5**, **Table 6** and **Table 7**.

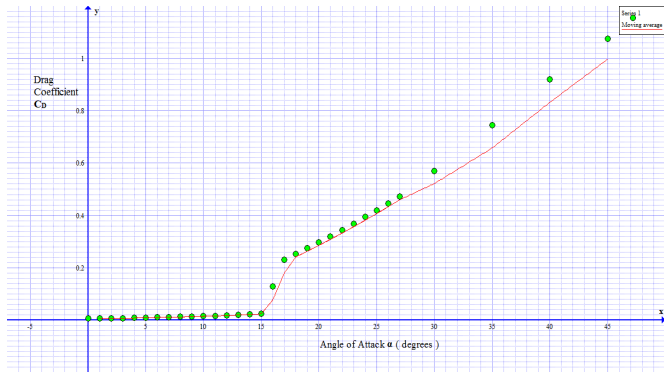


Figure 14: Graph of drag coefficient ( $C_D$ ) v/s angle of attack ( $\alpha$ )

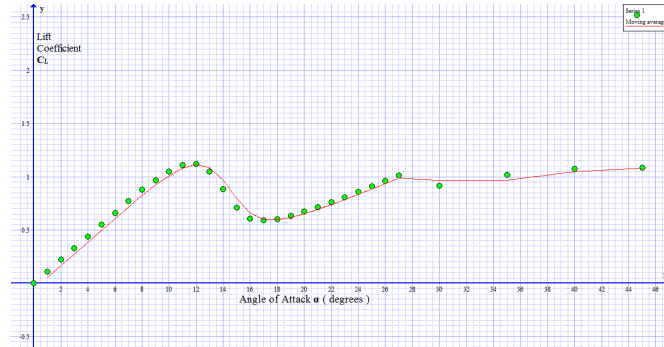


Figure 15: Graph of lift coefficient ( $C_L$ ) v/s angle of attack ( $\alpha$ )

The tangential force  $F_T$  provides the torque necessary for continuing the motion. It can be seen that this value changes at different azimuthal angles throughout the rotation. As a result, the torque produced and consequently the power is of fluctuating values.

Table 4: Values of angle of attack ( $\alpha$ ) for various combinations of azimuthal angle ( $\phi$ ) and tip speed ratio ( $\lambda$ )

$\phi$ (degree)			
$\rightarrow$	<b>104.5</b>	<b>112.6</b>	<b>131.9</b>
$\lambda \downarrow$			
<b>4</b>	14.4775	14.3235	12.5915
<b>2.6</b>	22.3938	22.62	21.0677
<b>1.5</b>	37.7669	39.6067	41.8103

Also, at  $\phi = 0^\circ$  and  $\phi = 180^\circ$ , the values of lift forces are zero. This indicates that it's only the drag force acting on the turbine, pushing it backwards. In such cases, the blade should move in opposite direction, but the presence of other blades, present at other azimuthal angles prevents that. Because of the three blade system, there is always at least one blade producing positive torque and keeping the rotor in motion!

At  $\phi = 104.5^\circ$

Tangential Force on rotor = 77.522 N (ref table 2)

Torque induced  $\tau = F_T \times R = 77.522 \times 0.7$

$$\therefore \tau = 54.26 \text{ N.m}$$

Angular Velocity  $\omega$  is given by  

$$\omega = \frac{2\pi N}{60}$$

where  $N$ = revolution per minute, here  $N= 327.40$  RPM

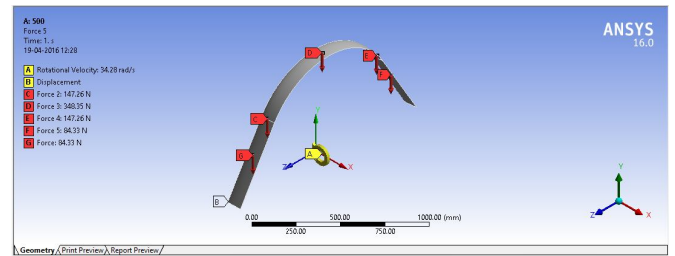


Figure 16: Force towards axis on aluminium blade for  $\phi = 104.5^\circ$

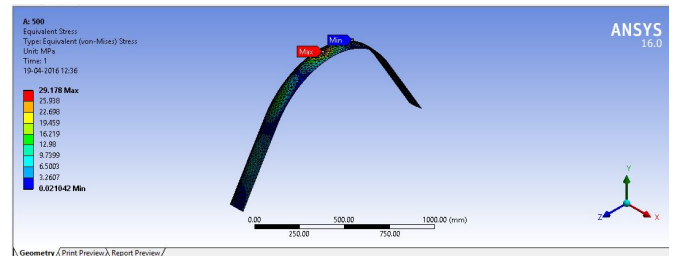


Figure 17: Equivalent stress on aluminium blade for  $\phi = 104.5^\circ$

Hence,  $\omega = 34.28 \frac{\text{rad}}{\text{sec}}$

Power produced =  $\tau \times \omega = 54.26 \times 34.28 = 1860.03$  Watts

Now, this value is comparatively high, but the rotor produces 1860.03 watts only at some time instant during one rotation. However, we can say that the turbine rotor must be producing sufficient power throughout its rotation as required by the streetlights.

### 4.3.2 Force analysis on Darrieus blade

The normal forces obtained in Table 5, 6, 7 for different azimuthal angles are applied on the blade and checked for overall stresses in ANSYS Static Structural with a rotation of 327.40 rpm.

Since the normal forces are high particularly at  $\phi = 104.5^\circ$  and  $\phi = 131.9^\circ$ . Hence, the analysis is done for these two values of  $\phi$ . As discussed earlier, the normal forces act in opposite direction for negative values of  $\alpha$ . The forces acting towards the axis are taken positive.

The results obtained are summarized in the **Table 8**.

**Table 5:** Calculation of forces for  $\lambda=4$

$\phi$ (degree)	$\alpha$ (degree)	$v_R$ (m/s)	$C_L$	$C_D$	$F_L$ (N)	$F_D$ (N)	$F_T$ (N)	$F_N$ (N)
0	0	30	0	0.0065	0	4.5162	-4.5162	0
180	0	18	0	0.0065	0	1.626	-1.626	0
104.5	14.4775	23.178	0.86	0.029	356.67	12.027	77.522	348.35
112.6	14.3235	22.493	0.91	0.02	355.43	7.812	80.363	346.31
131.9	12.5915	20.775	1.121	0.019	373.51	6.331	75.24	365.91

**Table 6:** Calculation of forces for  $\lambda=2.6$

$\phi$ (degree)	$\alpha$ (degree)	$v_R$ (m/s)	$C_L$	$C_D$	$F_L$ (N)	$F_D$ (N)	$F_T$ (N)	$F_N$ (N)
0	0	21.6	0	0.0065	0	2.341	-2.341	0
180	0	9.6	0	0.0065	0	0.462	-0.462	0
104.5	22.3938	15.16	0.756	0.344	134.13	61.03	-5.328	147.26
112.6	22.62	14.56	0.766	0.346	125.36	56.626	-4.05	137.5
131.9	21.0677	12.896	0.694	0.313	89.10	40.186	-5.47	97.59

**Table 7:** Calculation of forces for  $\lambda=1.5$

$\phi$ (degree)	$\alpha$ (degree)	$v_R$ (m/s)	$C_L$	$C_D$	$F_L$ (N)	$F_D$ (N)	$F_T$ (N)	$F_N$ (N)
0	0	15	0	0.0065	0	1.129	-1.129	0
180	0	3	0	0.0065	0	0.045	-0.045	0
104.5	37.7669	9.34	1.003	0.750	67.55	50.51	1.442	84.33
112.6	39.6067	8.951	1.04	0.818	64.327	50.59	2.032	81.81
131.9	41.8103	7.538	1.052	0.892	46.147	39.13	1.599	60.48

**Table 8:** Summary of results of force and stress calculation

Material	Force Direction	$\phi$	Maximum Normal Stress (MPa)	Maximum Equivalent Stress (MPa)	Maximum Total Deformation (mm)
Aluminium	Towards Axis	104.5	5.3612	8.3202	0.386
	Away From Axis	104.5	4.385	29.178	1.4523
	Towards Axis	131.9	6.475	11.56	0.2759
	Away From Axis	131.9	12.667	32.272	1.697
E- Glass Fibre	Towards Axis	104.5	3.661	11.18	0.278
	Away From Axis	104.5	9.2229	26.702	1.209
	Towards Axis	131.9	4.55	14.407	0.426
	Away From Axis	131.9	10.483	29.867	1.4512

## 5. DESIGN OF SAVONIUS TURBINE

The Savonius Turbine consists of two or three cylindrical blades as shown in **Figure 18**

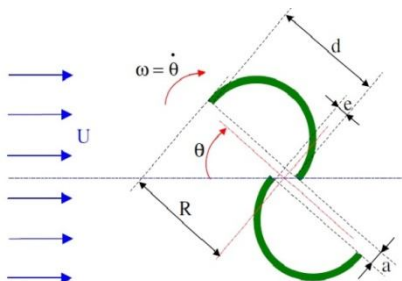


**Figure 18:** General geometric parameters of a Savonius turbine

### 5.1 Material considerations

The selection of materials depends on the materials selected for Darrieus blades, since the required properties are mostly the same. Hence, this design proceeds with both Aluminum alloy and E-Glass Fiber as blade materials.

### 5.2 Rotor Geometry

Since, it is a drag type rotor; no aerofoil section is required for the blades. Some important design parameters are:

- **Aspect ratio:** Aspect ratio is the ratio of total height (H) of the rotor to the rotor diameter (D). Theoretically



maximum efficiency is obtained when  $H= 2 D$ .

- **Number of blades:** It is seen [19] that two blades are more stable than three blades, in terms of performance.
- **Number of stages:** Increasing the number of stages of rotors on a turbine makes more height span of wind to be incident on the rotor. Note that the orientation of the ‘S’ shape formed by the blades on both stages are 90 degrees offset.
- **Overlap:** Overlap is the distance ‘e’ as shown in Figure 18.
- **Cover plates:** The cover plates are placed above and below the blades and to separate each stage.

Through the considerations of **shaft diameter = 100mm**, the design parameters selected are shown in **Table 9**. A CAD model of the design is shown in **Figure 19**

**Table 9:** Design parameters of Savonius turbine

Sr. No	PARAMETER	VALUE
1	Rotor height (H)	809 mm
2	Rotor Diameter (D)	400 mm
3	Blade Shape	Semicircular
4	Number of blades	2
5	Number of Stages	2
6	Height of each Stage (h)	400 mm
7	Bucket Diameter (d)	250 mm
8	Blade Thickness (t)	3 mm
9	Overlap (e)	103 mm
10	Cover plate Diameter (D <sub>c</sub> )	420 mm
11	Cover Plate Thickness (t <sub>c</sub> )	3 mm

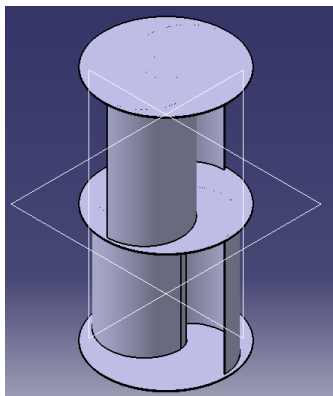


**Figure 19:** Savonius turbine complete CAD model

### 5.3 CFD analysis of Savonius blades

To understand the nature of drag pressure, an aerodynamic analysis is performed in CFD ANSYS FLUENT under static conditions.

Conditions of this two dimensional CFD analysis:

- The domain is of rectangular shape, of length= 20D and breadth = 10D
- The meshing is fine in the region around the rotor (sphere of influence of radius 550 mm )
- Boundary conditions-
  - Inlet velocity 6m/s, inlet gauge pressure 1 bar
  - Outlet gauge pressure 0 bar
  - Turbulent intensity 5%
  - No slip conditions throughout the domain
  - Wall motion stationary

[The Normal force is found to be maximum at 45 ° inclination [18]. Hence this analysis considers this instant.]

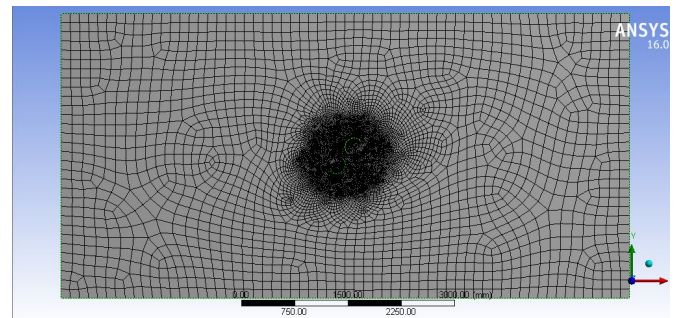


**Figure 20:** Meshing of Savonius rotor geometry in ANSYS FLUENT

### 5.4 Force analysis on Savonius blade

The maximum and minimum values of pressure are obtained at the concave and convex sides of the bottom blade.

$$P_{\max} = 28.1841 \text{ Pa (gauge pressure)}$$

$$P_{\min} = -57.208 \text{ Pa (gauge pressure)}$$

Thus, the total maximum pressure difference is given as  $\Delta P = P_{\max} - P_{\min} = (28.1841) - (-57.208) = 85.3921 \text{ Pa}$

Now, this pressure is active on the blade effective diameter. i.e.  $(d - e) = (250 - 103) = 147 \text{ mm}$

Hence, normal force acting per unit height is given by

$$fn = \Delta P \times (d - e)$$

$$\therefore fn = 85.3921 \times 0.147 = 12.5526 \text{ Nm}^{-1}$$

This force is applied on the blade and the blade is checked for stresses in ANSYS Static Structural.

[Note: The force is applied on the blade surface, although force acting throughout the surface varies. However, since the force considered is the maximum value, the design will be safe.]

For aluminium alloy, maximum equivalent stress = 2.9703 MPa

For E-Glass FRP material, maximum equivalent stress = 3.3177 MPa

Thus, it can be seen that Savonius blades made of both materials will not fail due to aerodynamic drag forces.

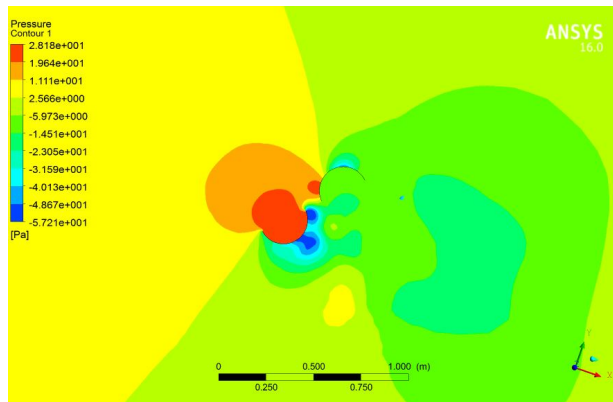


Figure 21: Pressure contour of Savonius rotor geometry in ANSYS FLUENT

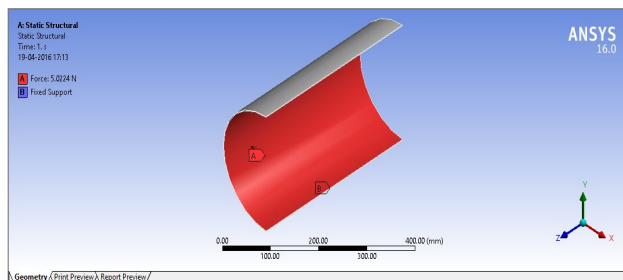


Figure 22: Analysis settings for Savonius aluminium blade in ANSYS Static Structural

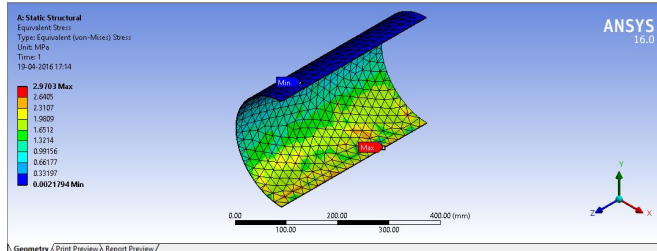


Figure 23: Equivalent stress distribution on Savonius aluminium blade in ANSYS Static Structural

## 6. CONCLUSION

On performing Stress analysis, both rotors show considerably safe results. This analysis can be succeeded by fatigue analysis and vibration analysis in future.

## ACKNOWLEDGEMENTS

The authors of this paper will like to thank the Department of Mechanical Engineering, Sardar Patel College of Engineering Mumbai for their extensive support and cooperation.

## REFERENCES

1. **Darrieus- Windmill**, Wikipedia.org
2. **PWV3- main**.,electronickits.com
3. IS : 1944 ( Parts 1 and 2 ) – 1970 , reaffirmed 2003

## **,Indian Standard Code of Practice for Lighting of Public Thoroughfares**

4. N. Lakshmanan et. al, **Basic wind speed map of India with long-term hourly wind data.**
5. Ramachandra T.V. and Shruthi B.V. ,**Wind energy potential in Karnataka, India** , Wind Engineering Volume 27, No. 6
6. Forecasts and Reports , **Wind Statistics**, Windfinder
7. Mazharul Islam, Firoz Uddin Ahmed et al, **Design Analysis of Fixed-pitch Straight-bladed Vertical Axis Wind Turbines with an Alternative Material**
8. Herbert J. Sutherland, Sandia National Laboratories, Wind Energy Technology Department , **A summary of fatigue properties of Wind Turbine Materials**
9. Manuel Franquesa Voneschen , **Brief Introduction to the Darrieus Wind Turbines** , Kleine Windradar, Berechnung und Konstruktion
10. David Hartman, Mark E. Greenwood, and David M.Miller, Owens Corning Corp. '**High Stength Glass Fibers**', 1996
11. Taher G. Abu-El-Yazied et. al. **Effect of Number of Blades and Blade Chord Length on the Performance of Darrieus Wind Turbine**, American Journal of Mechanical Engineering and Automation, January 2015
12. *Anonymous*, **Evaluation of Vertical Axis Wind Turbine Design for Stand Alone Application**
13. Thomas D. Ashwill, Timothy M. Leonard, **Development in Blade Shape Design for a Darrieus vertical Axis Wind Turbine**, Sandia Report SAND86-1085
14. Robert E. Sheldahl, Paul C. Klimas, **Aerodynamic Characteristics of Seven Symmetrical Airfoil Sections Through 180-Degree Angle of Attack for Use in Aerodynamic Analysis of Vertical Axis Wind Turbines**, Sandia Report SAND80- 2114
15. G. E. Reis, B.F. Blackwell, **Practical Approximations to a Troposkein by straight-line and circular –arc segments**, SAND74- 0100
16. M. Ragheb, **Optimal Rotor Tip Speed Ratio**
17. Wei Tong, **Wind Power Generation and Wind Turbine Design**
18. Paul G. Migilore, John R. Fritschen, Melior Corporation, California, **Darrieus Wind Turbine Airfoil Configuration**, Sub-Contract Report, June 1982
19. Rumana Hossain , Shaukat Ahmed , **A Study Of Aerodynamic Characteristics Of S-Shaped Savonius Rotor With Different Number Of Blades** , IJERT, ISSN : 2271-0181Jean-Luc Menet, Nachida Bourabaa ,Increase in the Savonius rotor's efficiency via a parametric investigation, *Ecole Nationale Superieure D'ingenieurs En Informatique Automatique Mecanique Énergetique Électronique De Valenciennes (Ensiame)*